

# GEOTHERMOBAROMETRY OF QUARTZPHYLLITES, ORTHOGNEISSES AND GREENSCHISTS OF THE AUSTRALPINE BASEMENT NAPPES IN THE NORTHERN ZILLERTAL (INNSBRUCK QUARTZPHYLLITE COMPLEX, KELLERJOCHGNEISS, WILDSCHÖNAU SCHISTS; TYROL, EASTERN ALPS)

Peter TROPPEL<sup>1</sup> & Andreas PIBER

Institute of Mineralogy and Petrography, Faculty of Geo- and Atmospheric Sciences, University of Innsbruck, Innrain 52f, A-6020 Innsbruck, Austria;

<sup>1</sup> Corresponding author, peter.tropper@uibk.ac.at

## KEYWORDS

Innsbruck Quartzphyllites  
Wildschönau Schists  
geothermobarometry  
Kellerjochgneiss  
Eo-Alpine

## ABSTRACT

The Innsbruck Quartzphyllite Complex (IQP), the Kellerjochgneiss (KG) and the Wildschönau Schists (WS) are part of the Austroalpine basement nappes north of the Tauern Window. These tectonic units occur in the northern Zillertal and in this study we present *P-T* data from all three units. The quartzphyllites of the IQP contain the mineral assemblage muscovite + albite + quartz + chlorite ± biotite, which is identical to the mineral assemblage in the WS. In the KG remnants of the magmatic precursor mineral assemblage K-feldspar + albite + previously Ti-rich biotite porphyroblasts are present. The Eo-Alpine mineral assemblage consists of muscovite + biotite + albite + chlorite + quartz ± stilpnomelane. *P-T* estimates obtained with multi-equilibrium geothermobarometry (THERMOCALC v.3.1, TWQ v.1.02) of a biotite-bearing quartzphyllite sample from the IQP range from 3.8 kbar to 5.9 kbar and 296 to 360°C. Lack of biotite in most of the samples of the IQP prohibits calculations of invariant intersections and consequently, only limiting pressure estimates of 3.5 kbar to 6 kbar in a temperature range of 300–400°C, based on the reaction paragonite + celadonite = muscovite + albite + clinoclinochlor + quartz + H<sub>2</sub>O, can be obtained. Greenschist intercalations of the eastern IQP contain the mineral assemblage amphibole + biotite + clinozoisite + albite + quartz. *P-T* conditions ranging from 325 ± 12°C to 360 ± 42°C and 4.5 ± 1.7 to 5.4 ± 1.8 kbar, based on the application of multi-equilibrium geothermobarometry, were obtained. Multi-equilibrium geothermobarometry of the KG yielded pressures of 4.1 kbar to 6.8 kbar at temperatures of 290°C to 370°C for the majority of all samples. Lack of biotite in most of the samples of the Wildschönau Schist hampered geothermobarometric calculations and only one sample yielded pressures of 4.9 kbar to 7.5 kbar and temperatures ranging from 300°C to 380°C. Stilpnomelane-muscovite-quartz geothermobarometry yielded *P-T* conditions of 4.3–5.7 kbar and 300–370°C for all three units. Based on similar microstructural evidence and previously published geochronological data it can be inferred that the *P-T* data of this investigation from these basement nappes in the northern Zillertal represent the Eo-Alpine metamorphic overprint. The data also indicate that the units of this investigation (KG, IQP, WS) underwent a similar Eo-Alpine tectonic evolution.

Die metamorphen austroalpinen Einheiten im nördlichen Zillertal sind der Innsbrucker Quarzphyllit (IQP), der Kellerjochgneis (KG) und die Wildschönauer Schiefer (WS). In dieser Arbeit präsentieren wir *P-T* Daten aus den drei Einheiten. Der IQP und der WS enthalten die Mineralparagenese Muskovit + Albit + Quarz + Chlorit ± Biotit. Im KG treten noch prä-alpine Relikte von K-Feldspat + Albit + Ti-reichen Biotitporphyroblasten auf. Die eo-alpine Mineralparagenese ist Muskovit + Biotit + Albit + Chlorit + Quarz ± Stilpnomelan. *P-T* Berechnungen mittels Multi-Equilibrium Geothermobarometrie (THERMOCALC v.3.1, TWQ v.1.02) einer biotit-führenden Probe aus dem IQP ergab 3.8 bis 5.9 kbar und 296 bis 360°C. Die Abwesenheit von Biotit in den meisten Quarzphyllitproben erlaubt nur die limitierende Anwendung der Reaktion Paragonit + Celadonit = Muskovit + Albit + Clinochlor + Quarz + H<sub>2</sub>O welche *P* von 3.5 kbar bis 6 kbar in einem *T*-Intervall von 300°C bis 400°C ergab. Grünschiefereinschaltungen im IQP mit der Paragenese Amphibol + Biotit + Klnozoisit + Albit + Quarz ergab *P-T* Bedingungen von 325±12°C bis 360±42°C und 4.5±1.7 bis 5.4±1.8 kbar. Multi-Equilibrium Geothermobarometrie des KG ergab *P* von 4.1 kbar bis 6.8 kbar bei *T* von 290°C bis 370°C. Das Fehlen von Biotit in den meisten Proben des WS erlaubte auch nur die Berechnung einer Biotit-führenden Probe, die *P* von 4.9 kbar bis 7.5 kbar und *T* von 300°C bis 380°C ergab. Die Anwendung der Stilpnomelan-Muskovit-Quarz Geothermobarometrie ergab *P-T* Bedingungen von 4.3–5.7 kbar und 300–370°C für alle drei Einheiten. Aufgrund der ähnlichen Mikrostrukturen in den bearbeiteten Proben und älteren geochronologischen Daten aus diesen Basementdecken lassen sich die *P-T* Daten dieser Untersuchung dem eo-alpinen Event zuordnen. Die ähnlichen *P-T* Daten aus den drei Einheiten lässt auch auf eine ähnliche eo-alpine tektonische Entwicklung schliessen.

## 1. INTRODUCTION AND GEOGRAPHICAL OVERVIEW

The investigated area is located in Tyrol (Austria) and is bordered by the Inntal to the north, the Wipptal to the West, the Zillertal to the East and the Navistal and the northern frame of

the Tauern Window to the South (Fig. 1). This study aims to provide petrological data of basement units, which were investigated in the frame of the TRANSALP-Project (Transalp Wor-

king Group, 2002). The aim of this project was the determination of the deep structure of the Alps between Bad Tölz (about 42 km in the South of Munich) and Treviso (about 25 km in the North of Venice) and its interpretation on the base of seismic data (Lüschen et al., 2004; Castellarin et al., 2006; Bleibinhaus and Gebrande, 2006). The focus of this study is the geothermobarometric investigation and interpretation of petrological data of the basement nappes of the Austro-Alpine realm in the northern Zillertal north of the Tauern Window. Since only few recently obtained quantitative *P-T* data are available from these units (Piber and Tropper, 2003a,b, 2007, 2010; Piber et al., 2009) this study aims to characterize the *P-T* history of these crystalline basement nappes, in conjunction with previously published geochronological data, which will lead to a concise insight into the geological evolution of this part of the Eastern Alps.

## 2. INTRODUCTION AND GEOLOGICAL OVERVIEW

The polymetamorphic crystalline basement north of the Tauern Window consists of orthogneisses (Kellerjochgneiss, KG/Schwazer Augengneiss), micaschists (Patscherkofel and Glungezer Crystalline Complex, PCC) and Paleozoic quartzphyllitic schists (Innsbruck Quartzphyllite Complex, IQP and Wildschönau Schists, WS) with intercalated carbonates (Schwarz Dolomite). These lithologies are in a hanging wall position in relation to the tectonic units of the Tauern Window. First intensive mapping investigations of the crystalline basement nappes

north of the Tauern Window were performed at the beginning of the 20<sup>th</sup> century by Ampferer and Ohnesorge (1918, 1924). Further extended and/or precise studies of the IQP were done in the second half of the 20<sup>th</sup> century by Schmidegg (1964), Gwinner (1971), Satir and Morteani (1978a, b), Hoschek et al. (1980), Satir et al. (1980), Mostler et al. (1982), Haditsch and Mostler (1982, 1983) and Roth (1983).

Due to its monotonous appearance, the IQP was treated as an undifferentiated unit over a long period. Haditsch and Mostler (1982, 1983) were the first to introduce a lithostratigraphic differentiation on the base of intercalated lithologies within the IQP. The most recent studies of Kolenprat et al. (1999) and Rockenschaub et al. (1999) confirm and complete Haditsch and Mostler's (1982, 1983) lithostratigraphic differentiation. In addition cooling ages of the quartzphyllites and Permian magmatic ages of different metaporphyrroids in the quartzphyllite basement are now available (Rockenschaub et al., 1999). According to the lithostratigraphy of Haditsch and Mostler (1982, 1983) the greenschist-quartzphyllite unit forms the stratigraphical lowest part of the IQP. This unit mainly consists of quartzphyllites with intercalated metabasic rocks. The metaporphyric rocks, which were thought to be of Ordovician age (Haditsch and Mostler, 1982, 1983), occur in the hangingwall. On top their so-called carbonate-sericite series, which consist of sericitic phyllites, chlorite-sericite-phyllites and quartzphyllites, occurs with intercalations of carbonate and dolomite marbles. This sequence is thought to be of Silurian age (Haditsch and

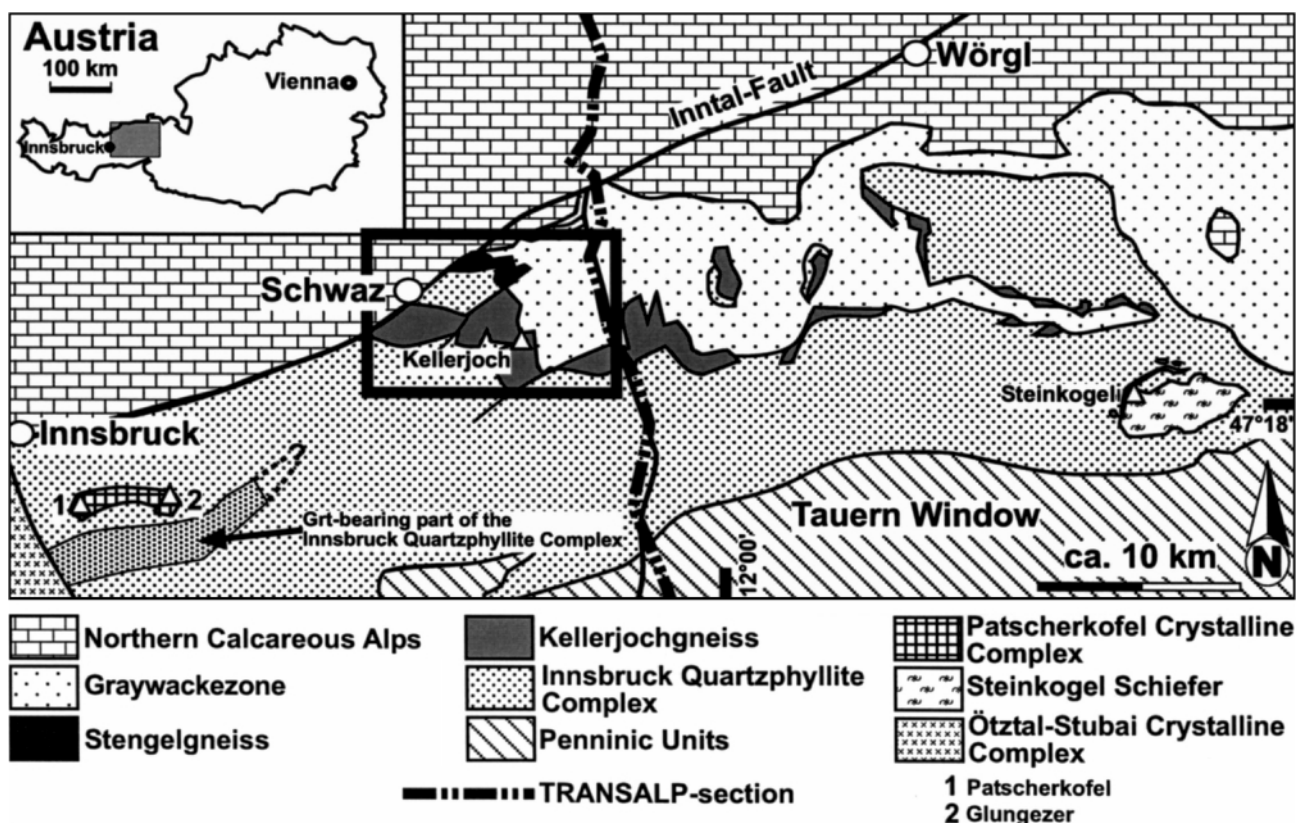


**FIGURE 1:** Geological overview of the Austroalpine basement nappes north of the Tauern Window. The black rectangle indicates the area of investigation. Note the TRANSALP section (stippled line) in the center of the image crosscutting the tectonic units.

Mostler, 1982, 1983). The highest stratigraphical sequence is the blackschist-carbonate-series. It consists of graphite-bearing phyllites and quartzphyllites with intercalations of iron-rich carbonates (dolomite marbles). Based on conodont stratigraphy, Höll and Maucher (1968) obtained late Silurian and early Devonian ages for the highest IQP parts. The most recent studies by Kolenprat et al. (1999), Rockenschaub et al. (1999) and Rockenschaub et al. (2003) helped to complete the stratigraphical footwall sequence of the IQP. In this sequence, micaschists, garnet-micaschists, paragneisses, amphibole-bearing greenschists and orthogneisses occur. Zircons, derived from metaporphyroids, yielded U/Pb ages, which can be interpreted as the result of a *T*-accentuated Permian event. These ages were also confirmed by Rb/Sr ages of white micas of the same lithologies (Rockenschaub et al., 2003). The eastern IQP, near the city of Schwaz, consists of a monotonous lithological sequence which is thought to represent the stratigraphically lowest sequence. The main lithology is quartzphyllite and greenschists frequently occur in the southern regions, while metacarbonates are nearly completely absent. Metaporphyroids, micaschists and garnet-micaschists as well as graphite-bearing phyllites also do not occur in this section of the IQP. Geothermobarometric data from the IQP are very sparse and are mostly based on the occurrence of index minerals such as chloritoid, garnet and biotite, which indicate a middle-greenschist-facies metamorphic overprint (Hoschek et al., 1980). A similar result was obtained by Sassi and Spiess (1992) based on muscovite unit cell data who obtained 3-4 kbar and 450°C. The most recent *P-T* data are from Dingeldey et al. (1997) who used multi-equilibrium methods (PTAX) and obtained *P-T* conditions of 3-4 kbar and 300-360°C.

The Kellerjochgneiss (KG, Schwaz Augengneiss) ranges from Schwaz in the West to Wildschönau, located in the South of Wörgl, in the East. The largest width of this crystalline basement nappe ranges up to 600 m in the area of Schwaz. Since the late 19<sup>th</sup> century (Pichler, 1868) the KG was the subject of geological investigations. In the second half of the 20<sup>th</sup> century the tectonic position of the KG was a subject of debates. Tollmann (1963, 1977, 1986) defined the KG as an Alpine nappe and attributed it together with the Steinkogelschiefer and Patscherkofel-Crystalline Complex (PCC) to the Middle Austroalpine unit, whereas other authors interpreted it to be the base of the inverted Innsbruck Quartzphyllite and thus to be of Lower Austroalpine origin (Schmidegg, 1954, 1964; Gwinner, 1971). According to the new tectonic subdivision of Schmid et al. (2004) the KG together with the IQP is part of the Upper Austroalpine Silvretta-Seckau nappe system. To unravel the geotectonic and metamorphic history of the Kellerjochgneiss detailed petrological studies were necessary (Piber, 2002, 2005; Piber and Tropper, 2010). Only few quantitative *P-T* data of the KG were obtained by Satir and Morteani (1978b) and Satir et al. (1980), who concluded, based on the Si-content of white micas, that *P* reached 5.3 kbar in the KG. Temperatures were estimated with stable isotope thermometry, based on <sup>18</sup>O-<sup>16</sup>O fractionations between phengite and quartz, and

yielded a temperature of 403°C. Satir and Morteani (1978b) interpreted these *P-T* conditions to represent the Variscan metamorphic event. Based on this interpretation, the authors concluded that the conditions of the Alpine metamorphic overprint did not exceed 350°C and 2-3 kbar. More recently Piber and Tropper (2003a,b, 2005, 2007, 2010) and Piber et al. (2009) published selected geothermobarometric data of the KG which yielded *P-T* conditions ranging from 4 to 8 kbar and 300-400°C, but a comprehensive geothermobarometric evaluation of the KG together with the IQP and WS is still missing.

The Wildschönau Schists (WS) are part of the Greywackezone, which extends over a distance of about 450 km from Schwaz in the West to the region of Ternitz (ca. 50 km in the Southeast of Vienna) in the East. The Noric Nappe of the Greywackezone forms the crystalline basement of the Tirolic nappe of the Northern Calcareous Alps (Ortner and Reiter, 1999). The metapelites and metapsammities of the WS mostly occur as grayish to grayish-green phyllites with varying amounts of quartz and feldspar. Locally the phyllites are intercalated by meta-siltstones. Several authors divide these phyllites stratigraphically into the lower and upper WS (Schönlaub, 1979; Reitz and Höll, 1991). These authors also postulate lower Ordovician ages for the lower WS, which is based upon intercalated mafic and ultramafic rocks. These ultramafic rocks are of early Ordovician age and range between 492 Ma and 454 Ma within a region between Schwaz in the West and Kitzbühel in the East (Schauder, 2002). Acidic magmatites in the vicinity of the WS mostly occur as metaporphyroids. Several samples of these acidic magmatites from the western region of Kitzbühel, were measured using single zircon U/Pb dating by Söllner et al. (1997) and yielded ages of 463±6 Ma, which corresponds to the middle Ordovician. The upper WS are accompanied by massive carbonates (Schwaz Dolomite, Spielberg Dolomite, Rettenstein Dolomite) and are divided into four tectonic units ("Faziesdecken" according to Schönlaub, 1980). Their age is still debated and lies probably between the late Ordovician and the late Silurian. In the western part of the Greywackezone the lithologies generally strike E-W. Geothermobarometric data from the western Greywackezone are only available from metabasic intercalations so far and yielded 4.5-8 kbar and 350-400°C (Collins et al., 1980).

Piber and Tropper (2010) identified six stages of deformation in the rocks of the IQP, KG and WS which could be correlated with the tectonic phases deduced by Froitzheim et al. (1994), Ortner et al. (1999) and Reiter (2000). The first stage (*D*<sub>1</sub>) is present as a relict foliation, observed only in microstructures of the KG. In the IQP the first deformation stage is also represented by a relict foliation occurring in isoclinal folds. The dominant foliation is represented in the second stage (*D*<sub>2</sub>), which is the result of a NW-SE-oriented compression. This main ductile deformation event also is expressed by the formation of a second generation of isoclinal folds. Associated shear bands indicate W-NW transport. The third ductile deformation stage (*D*<sub>3</sub>) leads to the formation of open folds most likely associated with a NE-SW contraction. The fourth stage (*D*<sub>4</sub>) is also cha-

acterized by open folds and an axial plane foliation, reflecting subsequent NNW-SSE compression. The last ductile stage ( $D_5$ ) produced semi-ductile kink bands, which crosscut the earlier deformation structures. The subsequent brittle deformation ( $D_6$ ) can be divided into four stages ( $D_{6a-d}$ ).

Based on geochronological and structural evidence from the three lithological units, it is possible to distinguish between pre-Alpine ( $D_1$ ) and Alpine ( $D_2 - D_6$ ) deformation structures (Piber and Tropper, 2010). The earliest stage of deformation ( $D_1$ ) can be linked with a pre-Alpine event (Variscan and/or Permian). The first stage of Eo-Alpine deformation ( $D_2$ ) can be correlated with the W-directed nappe stacking during the Early to Late Cretaceous. Geothermobarometric data indicate that the onset of this event during the Cretaceous took place under greenschist-facies conditions. The ongoing W-directed nappe transport led to intensive folding of all units and mylonitization of the KG. The subsequent nappe transport and stacking under progressive cooling accompanied by detachment of upper crustal parts during the Late Cretaceous led to the formation of shearbands within the basement nappes. This event was then followed by the extensional collapse during the latest Cretaceous ( $D_3$ ), which was succeeded by Paleogene collisional deformation events and the overriding of the Austroalpine nappe pile onto the Penninic units ( $D_4$ ). The early to middle Oligocene extension related to the onset of exhumation of the Tauern Window resulted in the last ductile deformation stage ( $D_5$ ). The last brittle stages ( $D_{6a-d}$ ) of the deformation sequence are probably associated with movements along the major fault lines in the area due to late Oligocene post-collisional shortening (Ortner et al., 1999; Reiter, 2000).

### 3. LITHOLOGICAL DESCRIPTIONS

*Quartzphyllites:* The IQP occur as low-grade metamorphic metapelites and metapsammites with different modal amounts of quartz and feldspar. Sericite-phyllites, chlorite-phyllites and mica-bearing quartzites rarely occur in this unit. Quartz segregations within the phyllites are lens-shaped and reach diameters ranging from a few cm up to several dm. The quartzphyllites of the WS exclusively occur in the NE of the study area as greenish-gray metapelites or metapsammites with varying amounts of quartz and feldspar. Some authors (Roth, 1983; Grasbon, 2001) subdivided this schist locally into a phyllitic-type and a sandy-type. These different types are closely related and often occur within a single outcrop. The quartzphyllites of the IQP and the WS are strongly foliated and exhibit poly-phase folding (Piber and Tropper, 2010). A visual differentiation between the phyllites of the WS and the IQP in an outcrop is nearly impossible.

*Greenschists* only occur in the southern parts of the eastern section of the IQP in the area of investigation. The diameter of these metabasic intercalations reaches up to several tens of meters, which have been found in the region of the uppermost Finsinggrund where they occur as ridges. These greenschist ridges can be traced over many hundreds of meters until they tectonically pinch out. The colour of these rocks is gray to

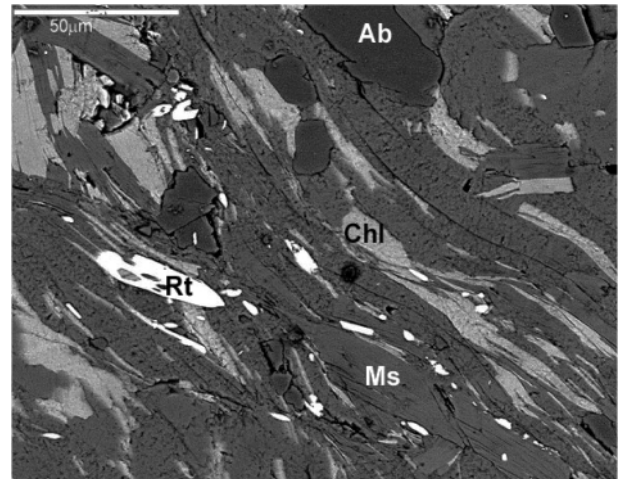


**FIGURE 2:** The backscattered electron (BSE) image of a sample of the IQP shows the mineral assemblage albite (Ab), chlorite (Chl), muscovite (Ms) and rutile (Rt) (sample A52).

green. Dark green colors are restricted to amphibole-bearing greenschists. The greenschists often are accompanied by thin layers of chlorite-phyllites. In the surrounding region of the Kellerjoch chlorite-phyllites with diameters of several cm occur.

*Orthogneisses:* The rocks of the KG occur as mylonitic augen-gneisses containing feldspar porphyroclasts with diameters of up to 3.5 cm. The color of these rocks is gray, grayish green or grayish brown. The different colors are due to different concentration of sheet silicates, mainly chlorite and biotite, or as a consequence of intensity of fracturing and accompanying grain-reduction of the rocks (Piber, 2002, 2005). Dark cataclastic sections within the Kellerjochgneiss are generally bound to zones of strong deformation.

### 4. PETROGRAPHY

*Quartzphyllites:* The mineral assemblage of the IQP is monotonous. Generally the main minerals of these rocks are muscovite, chlorite, albite-rich feldspar and quartz (Fig. 2; see Online Appendix Table 1). Locally, fine-grained biotites occur. Ac-

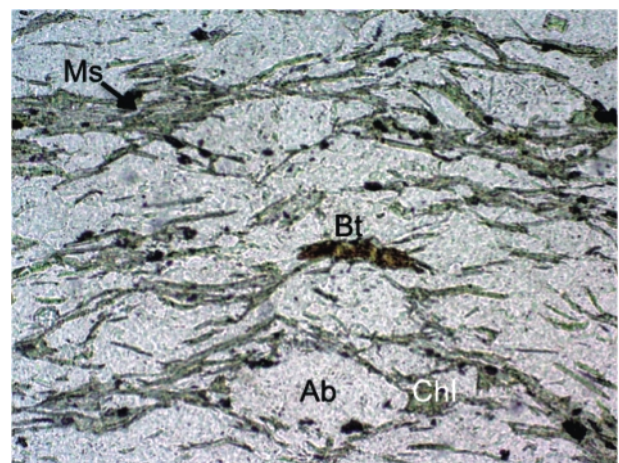


**FIGURE 3:** Photomicrograph of the mineral assemblage of muscovite (Ms), quartz (Qtz), albite (Ab) and chlorite (Chl) and biotite (Bt) of the WS (sample A-101, X Nichols, magnification 10x).

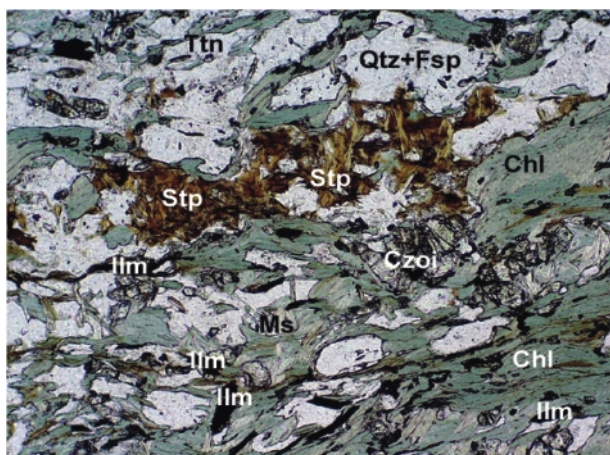


**FIGURE 4:** Photomicrograph of the mineral assemblage in the greenschists from the IQP showing albite (Ab), chlorite (Chl), clinozoisite (CzoI), muscovite (Ms), stilpnomelane (Stp), ilmenite (Ilm), titanite (Ttn) (sample A128, II Nichols, magnification 4x).

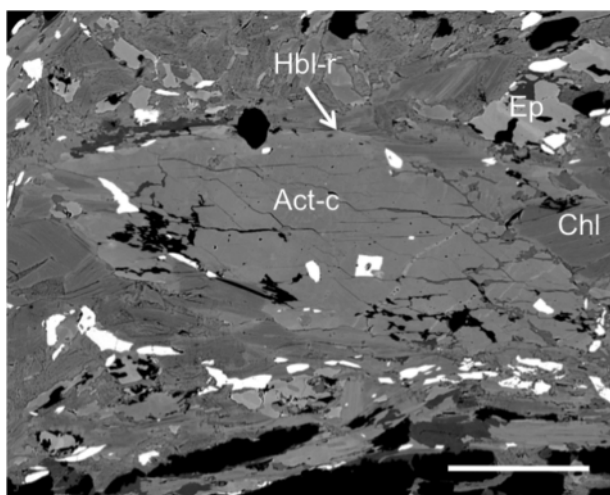


**FIGURE 5:** BSE image illustrating the chemical zonation of an amphibole with actinolite core (Act-c) and hornblende rim (Hbl-r). In the matrix chlorite (Chl) and epidote (Ep) occur (sample A-127b). Length of the scale bar is 100  $\mu$ m.



**FIGURE 6:** Photomicrograph of embayed quartz as an indicator of a shallow intrusion depth of the protolith of the KG (sample A-34, X Nichols, magnification 10x).

cessory minerals are calcite, rutile, ilmenite, tourmaline, zircon and graphite. In addition, ore minerals occur subordinately. The mineral assemblage of the WS is similar to the mineral assemblage of the IQP with the exception that the WS show slightly higher amounts of feldspar (Grasbon, 2001). The most common assemblage is muscovite, chlorite, albite-rich feldspar and quartz (Fig. 3; see Online Appendix Table 1). Biotite rarely occurs (Fig. 3). Accessory minerals are rutile, calcite, tourmaline, and Fe-hydroxide minerals such as limonite.

*Greenschists* within the IQP mainly exhibit the minerals chlorite, clinozoisite, albite-rich feldspar, titanite, calcite and biotite (Fig. 4; see Online Appendix Table 1). Some samples in addition contain amphibole, muscovite and stilpnomelane. Accessories are ilmenite, magnetite and zircon. The occurrence of amphibole is mostly restricted to lens-shaped rock bodies embedded to the greenschists. Amphiboles sometimes show evidence of prograde chemical zoning (Fig. 5). Rims are sometimes replaced by chlorite as a result of retrograde metamorphism. The mineral assemblage is: chlorite + clinozoisite + feldspar + titanite + calcite + biotite  $\pm$  muscovite  $\pm$  amphibole  $\pm$  stilpnomelane.

*Metacarbonates:* Since the metacarbonates lack petrologically relevant phases, only few samples were investigated. The investigated samples only consist of carbonates. Rarely muscovite occurs.

*Orthogneisses:* Remnants of granophyric intergrowth of K-feldspar and quartz are an indication for a shallow depth of intrusion of the KG. In addition, embayed quartzes within several samples of the gneiss are also an indication for shallow crystallization depths (Fig. 6). Roth (1983) assumed the embayment of quartz to be of mechanical origin, whereby deformation processes and leaching are responsible for a partly disruption of a quartz crystal. The main minerals of the KG are muscovite, biotite, chlorite, albite-rich feldspar and quartz (Fig. 7A; see Online Appendix Table 1). As a consequence of intensive deformation, many large feldspar individuals occur as fractured porphyroclasts. Sometimes magmatic K-feldspar and albite occur as single twinned phenocrysts. Quartz and feldspar are partly recrystallized. Former Ti-rich biotite from the magmatic protolith assemblage now contains abundant inclusions of Ti-bearing phases (sagenite grid of rutile crystals, Fig. 7B) (Piber, 2002, 2005). Only in rocks of the KG chemically zoned muscovites are found (Fig. 8). Muscovite shows in BSE images small (<5 mm) rims of a slightly brighter second generation of muscovite (Fig. 8). In addition, clinozoisite and stilpnomelane occur in several samples of the KG. Subordinately calcite appears locally. Accessory minerals are titanite, ilmenite, rutile, allanite, apatite and monazite.

## 6. MINERAL CHEMISTRY

Mineral compositions were measured with a JEOL X-8100 SUPERPROBE electron microprobe at the Institute of Mineralogy and Petrography of the University of Innsbruck. Operation conditions were 15 kV at a sample current of 20 nA, except for sheet silicates which were measured with a reduced sample

Sample	Unit	Nr. of calc.	KNMASH				KNFMASH			
			<i>P</i>	<i>2σ</i>	<i>T</i>	<i>2σ</i>	<i>P</i>	<i>2σ</i>	<i>T</i>	<i>2σ</i>
A-146	IQP	4	5.5	0.3	341	11	5	0.6	319	23
A-19	KG	8	4.9	1	297	19	6.5	1.3	350	22
A-56	KG	9	5.5	1	331	22	6.1	1.2	356	21
A-85	KG	8	6.8	1.1	335	23	7.8	1.3	365	22
A-87	KG	10	5.1	1.1	328	21	5.2	1.2	329	19
A-91	KG	10	5.2	1	310	20	6.5	1.2	348	20
A-98	KG	8	6.1	1.2	326	23	6.8	1.2	347	20
A-106	KG	9	6	1.1	337	23	5.9	1	367	20
A-120	KG	3	4.1	1.1	306	20	4.6	1.2	320	18

IQP: Innsbruck Quartzphyllite; KG: Kellerjochgneiss

**TABLE 1:** Results of the multi-equilibrium calculations of quartzphyllites and orthogneisses using THERMOCALC v.3.1

current of 10 nA and a rastered beam with a raster size between 2 and 5  $\mu\text{m}$  to prevent loss of alkaline elements. Natural and synthetic standards were used for calibration. Mineral formula calculations were performed with the programs MacAX (Holland, 1999; written comm.), Norm II (Ulmer, 2003; written comm.) and Hyperform96 (Bjerg et al., 1992). Amphibole formulae were calculated using the program AMPH-IMA97 (Mogessi et al., 2001).

**Muscovite:** In the eastern part of the IQP the Si contents of muscovites are low and lie between 3.06 and 3.17 a.p.f.u. with the exception of sample A-146, which is located at the tectonic base of the KG (see Online Appendix Table 2). Muscovites of this sample show clearly elevated Si contents of 3.32 to 3.36 a.p.f.u. In addition this sample contains biotite. The paragonite component [ $X_{\text{pa}} = \text{Na}/(\text{Na} + \text{K} + \text{Ca})$ ] and margarite component [ $X_{\text{mrg}} = \text{Ca}/(\text{Na} + \text{K} + \text{Ca})$ ] of all muscovites of the IQP never exceeds 5 mol.%. Muscovite rarely occurs in greenschists and was measured only in two samples of the eastern part of the IQP (A-113 and A-128). The Si contents lie between 3.24 and 3.33 a.p.f.u. Muscovites of the greenschists show a distinctly higher celadonite component as muscovites in the adjacent quartzphyllites. Muscovite is also very common in the KG (Online Appendix Table 2). The diameter of muscovites strongly varies as a consequence of mylonitization and synkinematic mineral growth and the white micas are generally aligned with the penetrative foliation. In addition several samples contain chemically zoned muscovites where higher Na as well as Si (Fig. 9) contents are seen in the rims. Rims are usually very thin with  $<5\mu\text{m}$ . The Si contents of these rims are high and lie between 3.27 and 3.52 a.p.f.u. (Fig. 7). The muscovites of the WS occur as fine-grained crystals, which are aligned in the penetrative foliation. Muscovites do not display any chemical zonation. The Si contents of the muscovites lie between 3.13 and 3.43 a.p.f.u. for the biotite-bearing sample. Paragonite component ( $X_{\text{pa}}$ ) and margarite component ( $X_{\text{mrg}}$ ) are below 1 mol.% (Online Appendix Table 2).

**Biotite:** Biotites of sample A-146 from the eastern part of the IQP shows  $\text{Fe}/(\text{Fe}^{2+} + \text{Mg})$  ratios of 0.67 to 0.68 (see Online Appendix Table 3). Ti contents of these biotites are low and only

range from 0.11 to 0.12 a.p.f.u. Biotites only rarely occur within the greenschists. They are often replaced by chlorite as a consequence of the retrograde metamorphic overprint. The

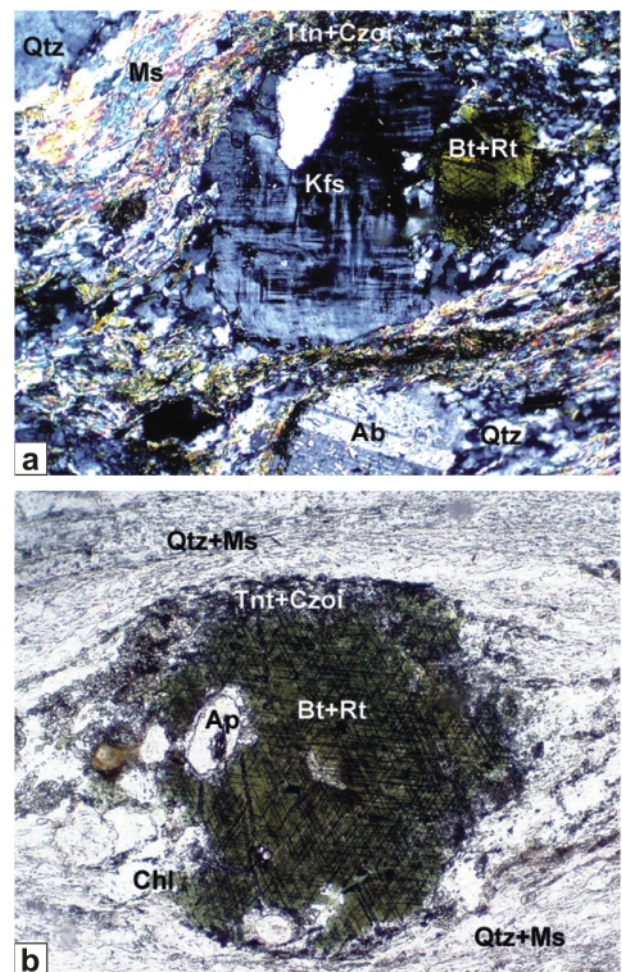


**FIGURE 7:** Photomicrograph (X Nichols) of the characteristic mineral assemblage of the KG. A: relic K-feldspar (Kfs) and albite porphyroblasts, magmatic biotite (Bt) with rutile (Rt) inclusions occurring as sa-genite grid and chlorite (Chl) and muscovite (Ms), sample A-56. B: close-up of the biotite porphyroblasts showing at the rim of the old biotites, titanites (Ttn) and clinozoisites (Czo) (Il Nichols, magnification 4x) (sample A-19).

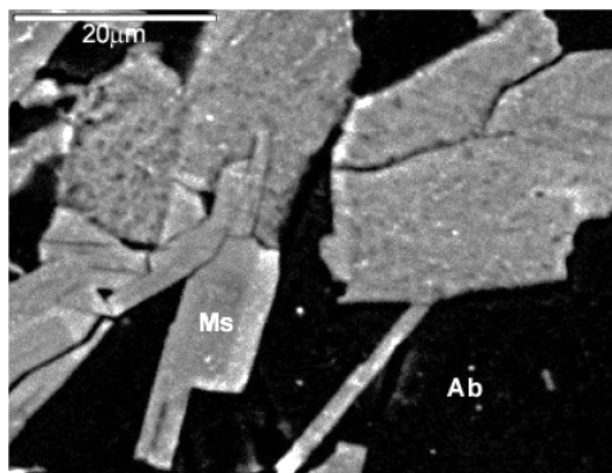


**FIGURE 8:** Backscattered electron (BSE) image of a zoned muscovite from the KG showing bright rims (sample A19).

Fe/(Fe<sup>2+</sup>+ Mg) ratio is between 0.29 and 0.46. Ti contents range from 0.08 to 0.11 a.p.f.u. (Online Appendix Table 3). Biotites in the KG also show different grain sizes. A first, most likely magmatic generation occurs as large porphyroblasts containing well-developed sagenite patterns. This biotite generation shows very high Ti contents ranging up to 5.55 wt. % TiO<sub>2</sub>, which is due to contamination by small rutile needles intergrown with biotites. The second biotite generation, which is arranged in the penetrative foliation, shows lower Ti contents ranging from 1 to 3 wt. % TiO<sub>2</sub> (Online Appendix Table 3). Al<sub>tot</sub> contents range from 1.39 to 1.47 a.p.f.u. Similar to the white micas, biotites in the WS are also arranged within the penetrative foliation. They show Fe/(Fe<sup>2+</sup>+Mg) ratios ranging from 0.54 to 0.57. Al<sub>tot</sub> contents vary from 1.38 to 1.50 a.p.f.u. and Ti contents are low and range from 0.07 to 0.13 a.p.f.u. (Online Appendix Table 3).

*Chlorite:* Chlorites of the IQP are Fe-rich with a Fe/(Fe<sup>2+</sup>+Mg)

ratio of 0.64-0.66 (see Online Appendix Table 4). The biotite-bearing sample A-146, located adjacent to the tectonic border to the KG, shows slightly higher Fe contents with a Fe/(Fe<sup>2+</sup>+Mg) ratio of 0.67±0.05 (Online Appendix Table 4). Al<sub>tot</sub> contents of chlorites from the IQP lie at values of 2.75 to 3.01 a.p.f.u. According to the chemical classification of Hey (1954) the chlorites are rhipidolites. Chlorite is also one of the main minerals in the greenschists. According to the nomenclature of Hey (1954) these chlorites are classified as rhipidolites and pycnochlorites with a Fe/(Fe<sup>2+</sup>+Mg) ratio of 0.43-0.44 (Table 4). The Al<sub>tot</sub> content shows values lying between 1.97 and 2.61 a.p.f.u. (Online Appendix Table 4). Chlorite in the KG is also very Fe-rich with a Fe/(Fe<sup>2+</sup>+Mg) ratio of 0.64-0.68. Al<sub>tot</sub> contents lie between 2.20 and 2.60 a.p.f.u. According to the chlorite nomenclature of Hey (1954) these chlorites are classified as rhipidolites and brunsvigites. Chlorite is also common in the WS and is aligned within the penetrative foliation. The Fe/(Fe<sup>2+</sup>+Mg) ratio lies between 0.54 and 0.56. Al<sub>tot</sub> contents range from 2.46 to 2.61 a.p.f.u. (Online Appendix Table 4).

*Feldspar:* All feldspars from the IQP are almost pure albite (Ab<sub>99-100</sub>) (see Online Appendix Table 5). Feldspars of the greenschists of the IQP also contain very high amounts of albite-component (Ab<sub>98-100</sub>). In addition, nearly pure K-feldspar (Kfs<sub>98-100</sub>) occurs in most of the greenschist samples. Several feldspars of the KG occur as porphyroclasts with diameters of up to 3.5 cm. Large magmatic phenocrysts (Kfs97-100) are partly replaced by newly grown albite, mostly along fractures and at the rims. These nearly pure albites contain an anorthite component (X<sub>An</sub>) <3 mol.%. Smaller newly grown feldspar individuals are mainly albites (Ab<sub>98-100</sub>) and the amount of K-feldspar is less than <1 mol.% (Online Appendix Table 5). Similar to the IQP, feldspars in the WS are also pure albites (Ab<sub>98-100</sub>). The anorthite and the K-feldspar component (X<sub>An</sub>, X<sub>Kfs</sub>) never exceeds 1 mol.% (Online Appendix Table 5).

*Stilpnomelane* occurs in the greenschists of the IQP and the KG and shows a large variation in the Fe/(Fe<sup>2+</sup>+Mg) ratios of 0.14-0.41 (Online Appendix Table 4). Mn contents range from 0.07 to 0.14 a.p.f.u. (Online Appendix Table 6).

*Amphibole:* Amphiboles of the greenschists intercalated in the IQP are chemically zoned (Fig. 4). The cores of the amphiboles are poor in Al with contents lying between 1.00

Sample	Unit	Nr. of calc.	P	2σ	T	2σ
A-146	IQP	2	4.8	1.2	321	28
A-127b	GRS/IQP	3	4.5	1.7	340	40
A-19	KG	3	5.3	1.4	309	30
A-56	KG	3	5.1	1.2	319	28
A-91	KG	2	4.5	1.4	300	30
A-101	WS	4	4.9	1.2	324	30

IQP: Innsbruck Quartzphyllite; KG: Kellerjochgneiss; WS: Wildschönau Schists; GRS: greenschists

**TABLE 2:** Results of the average PT calculations using THERMOCALC v.3.1

Sample	Unit	Nr. of calc.	CNMASH				CNFMASH-1				CNFMASH-2			
			P	2σ	T	2σ	P	2σ	T	2σ	P	2σ	T	2σ
A-127b	IQP	2	5.4	1.8	359	42	6.2	1.9	390	46	6.1	2	395	53
N88-1	IQP	2	6	0.5	325	12	-	-	-	-	6.8	0.6	355	16

IQP: Innsbruck Quartzphyllite

**TABLE 3:** Results of the multi-equilibrium calculations of greenschists using THERMOCALC v.3.1

and 4.00 wt. %  $\text{Al}_2\text{O}_3$  (Online Appendix Table 7). Rims are richer in  $\text{Al}_2\text{O}_3$  and  $\text{Na}_2\text{O}$  and the Al contents range from 3.98 to 11.62 wt. %  $\text{Al}_2\text{O}_3$  and Na values lie between 0.85 and 2.41 wt. %  $\text{Na}_2\text{O}$  (Online Appendix Table 7). According to the classification of Leake et al. (1997) the cores can be classified as actinolites and the rims can be classified as magnesio-hornblendes (Fig. 10). The Na contents on the B-position of the amphibole cores lies at  $<0.25$  Na a.p.f.u. and increase up to 0.61 Na a.p.f.u. in the rims. Al(IV)-content also increase from core to rim ranging from  $<0.26$  to 1.52 a.p.f.u. (Online Appendix Table 7).

**Clinozoisite:** Clinozoisites are important rock-forming minerals in the greenschists of the IQP. Clinozoisites are  $\text{Fe}^{3+}$ -rich with  $\text{Fe}^{3+}$  contents ranging from 0.70 to 0.92 a.p.f.u. (Online Appendix Table 8). The Al contents lie between 2.06 and 2.20 a.p.f.u.

**Titanite:** Titanite occurs as accessory mineral in the greenschists of the IQP. The Ti contents lie between 33.21 wt.% and 40.20 wt. %  $\text{TiO}_2$  (Table 8). Ti can be substituted by Al and  $\text{Fe}^{3+}$  and the Al contents range from 0.68 wt.% up to 4.03 wt. %  $\text{Al}_2\text{O}_3$  and  $\text{Fe}^{3+}$  contents range from 0.53 wt.% to 4.00 wt. %  $\text{Fe}_2\text{O}_3$ .

## 7. GEOTHERMOBAROMETRY

Multi-equilibrium calculation methods using THERMOCALC v.3.1 (Holland and Powell, 1998) and TWQ v.1.02 (Berman, 1988) were applied to selected samples. The computations with THERMOCALC v.3.1. were two-fold: 1.) calculations in the chemical subsystems  $\text{K}_2\text{O}-\text{Na}_2\text{O}-\text{FeO}-\text{MgO}-\text{Al}_2\text{O}_3-\text{SiO}_2-\text{H}_2\text{O}$  (KNFMASH) and  $\text{K}_2\text{O}-\text{Na}_2\text{O}-\text{MgO}-\text{Al}_2\text{O}_3-\text{SiO}_2-\text{H}_2\text{O}$  (KNMASH) were done using selected invariant points as given in the Online Appendix; and 2.) the average PT mode was used. In latter approach an independent set of reactions is displaced in order to coincide with the P-T conditions of formation and these displacements are mainly made by varying the activities of the end-members of the minerals, in proportion to their uncertainties (see Powell and Holland, 1988, 1994). TWQ v.1.02 calculations were performed in the system  $\text{K}_2\text{O}-\text{Na}_2\text{O}-\text{FeO}-\text{MgO}-\text{Al}_2\text{O}_3-\text{SiO}_2-\text{H}_2\text{O}$  (KNFMASH) with the dataset Jun92.gsc (Berman, 1992, written comm.) as well as the extended dataset of Massonne (1997, written comm.). The extensions of the dataset by Massonne (1997, written comm.) are based on the incor-

Sample	Unit	Nr. of calc.	<i>P</i>	$2\sigma$	<i>T</i>	$2\sigma$
<b>Berman (1992)</b>						
A-19	KG	6	6.3	1	307	10
A-56	KG	7	6.4	0.8	321	6
<b>Massonne (1997)-1</b>						
A-19	KG	4	5.8	0.8	294	34
A-56	KG	3	6	1.4	292	54
A-85	KG	3	5.2	2	297	58
A-91	KG	6	5.6	1.2	303	36
A-146	IQP	3	5.7	0.2	300	12
A-101	WS	4	4.9	0.8	298	42
<b>Massonne (1997)-2</b>						
A-19	KG	11	6.4	0.8	308	4

IQP: Innsbruck Quartzphyllite; KG: Kellerjochgneiss; WS: Wildschönau Schists; Massonne (1997)-1: no stilpnomelane; Massonne (1997)-2: + stilpnomelane

**TABLE 4:** Results of the multi-equilibrium calculations in the system KNFMASH using TWQ Berman (1992)

poration of Mg-Al- and Fe-Al-celadonite based on the thermodynamic data by Massonne and Szpurka (1997) as well as small additional modifications as outlined in Willner et al. (2000) and Massonne and Kopp (2005). Quantifications of the *P-T* conditions were done using the software INTERSX which computes an average *P* and *T* from all intersections between curves, weighted towards those equilibria with the highest  $\Delta S$ ,  $\Delta V$  and smallest  $\ln K$ , and which intersect most orthogonally (Berman, 1991). All multi-equilibrium calculations have to be performed assuming  $a(\text{H}_2\text{O}) = 1$ , due to the absence of additional constraints on  $a(\text{H}_2\text{O})$  and the small number of phase components. To validate the assumption of  $a(\text{H}_2\text{O}) = 1$  the empirical  $\text{H}_2\text{O}$ -independent stilpnomelane-thermobarometer by Currie and van Staal (1999) was applied to stilpnomelane-bearing samples and the results were compared with the *P-T* results derived from TWQ v.1.02 using the dataset of Massonne (1997, written comm.) including the assemblage stilpnomelane + celadonite + chlorite + quartz. The mineral reactions associated with these calculations are given in the Online Appendix.

The mineral assemblage of most samples from the IQP is muscovite + chlorite + albite-rich plagioclase + quartz and only one metapelitic sample contains the mineral assemblage

Sample	Unit	Nr. of calc.	<i>T</i>	$1\sigma$	<i>P</i>	$1\sigma$
A19	KG	14	291	35	5.4	1.07
A34	KG	18	351	42	5.7	0.64
A119	KG	3	401	59	4.8	1.62
A120	KG	2	354	3	5.2	0.01
A128	GRS/IQP	8	368	62	4.3	1.02

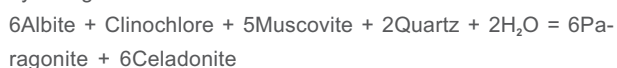
IQP: Innsbruck Quartzphyllite; KG: Kellerjochgneiss; WS: Wildschönau Schists; GRS: greenschist

**TABLE 5:** IQP: Innsbruck Quartzphyllite; KG: Kellerjochgneiss; WS: Wildschönau Schists; GRS: greenschist

muscovite + albite + chlorite + quartz + biotite. The KG contains at least two stages of mineral growth from different metamorphic events within different microdomains as a result of the polymetamorphic history of this lithology. To ensure that the *P-T* results correspond to the main (e.g. the latest) metamorphic event, which is associated with the penetrative foliation, chemical analyses were derived from muscovite rims from small micro-domains showing clear textural relationships among the minerals.

### 7.1 RESULTS OF MULTI-EQUILIBRIUM GEOTHERMOBAROMETRY

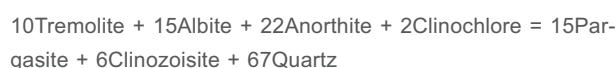
**THERMOCALC v.3.1:** Most of the metapelite samples of the IQP from the eastern area only contain the mineral assemblage muscovite + chlorite + albite + quartz which restricts geothermobarometric calculations to pressure estimates at an assumed temperature space. These estimates were derived by using the reaction:



calculated over a *T* range between 280–400°C. The temperature range was calculated using the Fe-Mg cation exchange reaction between chlorite and biotite. The lowest pressure limits at 280°C yielded 4.5 kbar to 5.1 kbar, pressures between 5.9 kbar to 6.6 kbar could be obtained at an upper temperature limit of 400°C. The variations in pressure are due to slight chemical variations of the paragonite component in muscovite. One biotite-bearing metapelite sample (A-146) could be used for multi-equilibrium calculations with THERMOCALC v3.1. These calculations resulted in pressures of 5.5±0.3 kbar at a *T* of 341±11°C in the system KNMASH (Table 1). Calculations of the best-fitted intersections in the system KNFMASH applying the end-members muscovite-paragonite-celadonite-phlogopite-clinocllore-albite-quartz-H<sub>2</sub>O yielded pressures of 5.0±0.6

kbar at a temperature of 319±23°C (Table 1). Calculations using the average *PT* mode yielded *P-T* conditions of 4.8±1.2 kbar and 321±28°C (Table 2).

Additional geothermobarometric information could be derived from calculating invariant points in chemical sub-systems with THERMOCALC v3.1 by using the greenschist samples containing the mineral assemblage amphibole + biotite + chlorite + clinzoisite + plagioclase + quartz (Table 3). The chemical analyses of the assemblage were taken from micro-domains and coexisting minerals to assure equilibrium. An invariant point was calculated in the H<sub>2</sub>O-involving system CNMASH and two invariant points were calculated in the system CNFMASH by using the end-members albite-anorthite-clinocllore-daphnite-tremolite-pargasite-ferroactinolite-clinzoisite-phlogopite-annite-quartz-H<sub>2</sub>O. The calculations yielded a spread in *P* at a considerable *T* range and the samples A127-b and N88-1 yielded pressures ranging from 5.4 kbar to 6.8 kbar. Pressure shifts are mostly the result of variations in the activity of the pargasite component, which implies rising pressures with higher contents of AlVI and Na(B) in amphibole. The reactions used are:



and



Temperature was determined by the Fe-Mg exchange reactions between amphibole-chlorite-biotite:



and



Calculations using the average *PT* mode yielded 4.5±1.7 kbar and 340±40°C.

*P-T* results of the Kellerjochgneiss with THERMOCALC v.3.1 were restricted to calculations with the assemblage muscovite + biotite + chlorite + feldspar + quartz (Table 1). *P-T* estimates were obtained by calculating intersections in the system KNMASH and KNFMASH and with the average *P-T* mode in the system KNFMASH with the application of the end-members muscovite-celadonite-paragonite-annite-phlogopite-albite-clinocllore-daphnite-quartz-H<sub>2</sub>O. Invariant points were calculated and yielded *P* between 4.1 kbar and 6.8 kbar at temperatures ranging from 310 to 370°C (Table 1). Uncertainties in pressure and temperature are also the results due to differences in the paragonite component in muscovite. Deviations in *P* reach up to maximum values of 2.4 kbar due to compositional variations of muscovite within one sample. Computations using the THERMOCALC v.3.1 average *PT* mode yielded *P* ranging from 4.5 kbar to 5.3 kbar at *T* ranging from 300°C to 320°C (Table 2).

Geothermobarometric results from the WS with the program THERMOCALC v.3.1 were only possible with one sample (sample A-101). Sample A-101 contains the mineral assemblage muscovite + biotite + chlorite + plagioclase + quartz. The *P-T* results computed with the average *PT* mode yielded

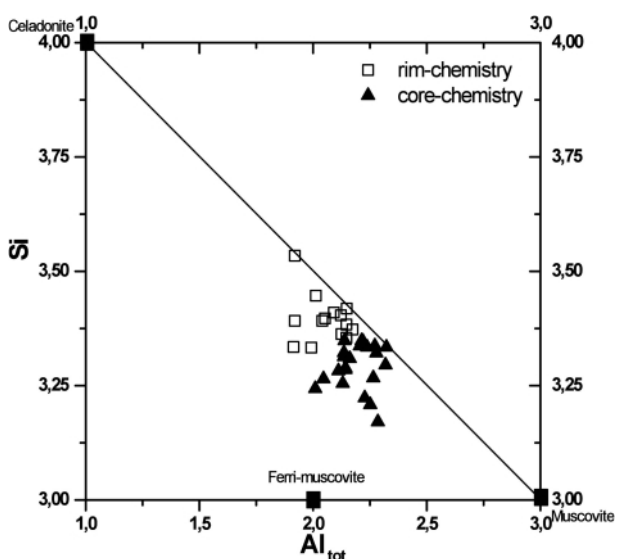


**FIGURE 9:** Chemical variation in Si vs. Al<sub>tot</sub> of the zoned muscovites from the KG. The open squares represent rim analyses and the black triangles core analyses (sample A-19).

4.9±1.2 kbar and 324±30°C (Table 2).

TWQ v.1.02: Intersections within the H<sub>2</sub>O-present system KFMASH were obtained for the IQP by using the biotite-bearing sample A-146 and applying TWQ v.1.02 with the dataset of Berman (1992, written comm.) and the extended data set of Massonne (1997, written comm.) as shown in Table 4. Chlorite end-members activities were used according to the ideal ionic model according to Powell (1978). Intersections yielded *P-T* conditions for the IQP of 5.7±0.2 kbar and 300±12°C (Table 3).

*P-T* results of the KG with the multi-equilibrium program TWQ v.1.02 were also calculated with the datasets of Berman (1992, written comm.) and Massonne (1997, written comm.). Average *P-T* data were obtained in the system KNFMASH (Table 3). The assemblage used for the calculations was muscovite + biotite + chlorite + plagioclase + quartz + H<sub>2</sub>O. Additional calculations of stilpnomelane-bearing samples of the Kellerjochgneiss were used for calculating intersections incorporating stilpnomelane by applying the dataset of Massonne (1997, written comm.) in the system KNFMASH and the assemblage stilpnomelane + muscovite + chlorite + plagioclase + quartz + H<sub>2</sub>O (Table 3). Results computed with TWQ v.1.02 with the data set of Berman (1992, written comm.) in the system KNFMASH yielded *P* ranging from 5.2 kbar to 6.4 kbar at *T* of 290 to 320°C (Fig. 11, Table 4). Pressure shifts within a sample are the result of reactions involving muscovite and the celadonite component and the variation of muscovite composition lead to maximum deviation of ±1.1 kbar within a sample. The calculations were done using the ideal ionic activity models for chlorite and biotite. The shift in *P-T* due to different chlorite activity models (ideal ionic, ideal molecular according to Powell, 1978; Evans, 1990, Holland et al., 1998) resulted in <1 kbar and <10°C. The shift due to different biotite activity models (ideal ionic, McMullin et al., 1991) is slightly higher with <1.5 kbar and <20°C.

TWQ v.1.02 calculations of the WS were performed with the data set of Massonne (1997, written comm.). For *P-T* estimations the assemblage muscovite + biotite + plagioclase + quartz + H<sub>2</sub>O were used. Clinocllore and daphnite activity was calculated according to the ideal ionic model according to Powell (1978). The calculations yielded *P* of 4.9±0.4 kbar at *T* of 300±21°C. *P* deviations correspond to a varying celadonite component and lie within a range of 0.3 kbar.

## 7.2 RESULTS OF STILPNO-MELANE GEOTHERMOBAROMETRY

Computations with the BASIC program stilp.mod2 by Currie and van Staal (1999) were applied to the assemblage stilpnomelane + musco-

vite + chlorite + quartz. Stilp.mod2 calculates *P-T* conditions based on the intersection between the two reactions  
 89Daphnite + 131Fe-celadonite + 190Quartz = 96Stilpnomelane + 7Muscovite  
 Amesite + Mg-celadonite = Clinocllore + Muscovite

which allows the simultaneous estimation of *P* and *T* in the H<sub>2</sub>O-absent system KFMASH. Standard deviations are fixed with 0.5 kbar in pressure (1 $\sigma$ ) and 25°C in temperature (1 $\sigma$ ). Sample A-128, a greenschist of the IQP, was used and *P-T* conditions of 4.3±1.1 kbar and 368±68°C were obtained (Table 5). Calculations of KG samples using the assemblage stilpnomelane + muscovite + chlorite + quartz yielded *P* estimates in the range of 4.8 to 5.7 kbar and a *T* range between 290 and 400°C. These H<sub>2</sub>O-independent *P-T* conditions nicely confirm the H<sub>2</sub>O-involving multi-equilibrium calculations assuming a(H<sub>2</sub>O) = 1.

## 8. DISCUSSION

### 8.1 COMPARISON OF THE GEOTHERMOBAROMETRIC RESULTS WITH PREVIOUS *P-T* DATA

The results of this study show that the *P-T* data obtained with different thermodynamic databases and methods yield consistent results and converge at ca. 5-7 kbar and 300-400°C. Previous *P-T* data from the IQP by Hoschek et al. (1980), Sassi and Spiess (1992) and Dingeldey et al. (1997) yielded *P-T* conditions of 3-4 kbar and 300-450°C, which are in good agreement with the data from our investigation. The only older *P-T* data of the KG were obtained by Satir and Morteani (1978a, b) and Satir et al. (1980) so far, who concluded that *P* reached 5.3 kbar and *T* reached a maximum of 400-410°C in the KG. Due to the absence of unambiguous Eo-Alpine ages, Satir and Morteani (1978) interpreted these *P-T*-conditions to represent the Variscan metamorphic event. Based on this interpretation and the available age data, the authors concluded that the conditions of the Alpine metamorphic overprint did not exceed

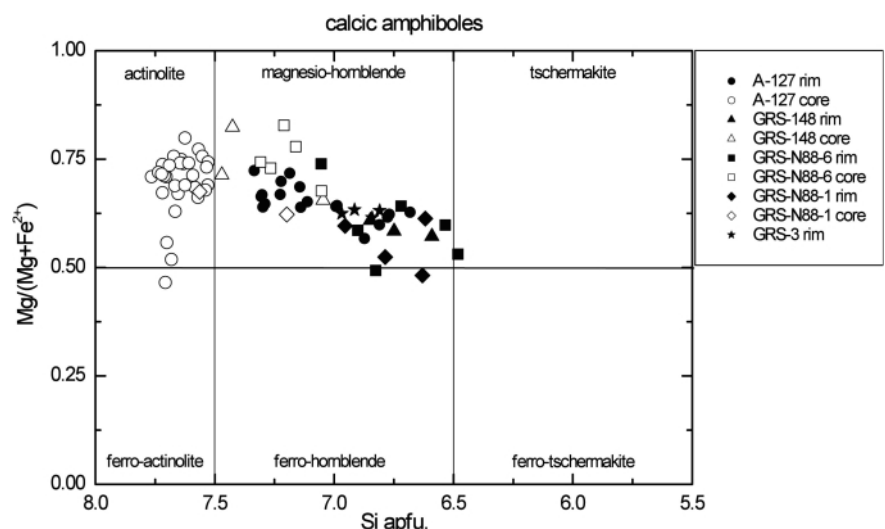


FIGURE 10: Chemical classification of amphiboles of the IQP according to the classification of the calcic amphiboles after Leake et al. (1997).

lower greenschist-facies conditions of 350°C and 2-3 kbar. Geothermobarometric results from recent studies and this investigation yielded pressures of 4.0 to 7 kbar and temperatures between 290 and 400°C for the KG and the IQP (Piber and Tropper, 2003a,b, 2005, 2010; Piber et al., 2009). Our data are also consistent with the previous semi-quantitative *P-T* estimates by Collins et al. (1980) who obtained 350-400°C and 3-8 kbar.

## 8.2 CORRELATION BETWEEN THE GEOTHERMOBAROMETRIC RESULTS AND THE EXISTING GEOCHRONOLOGICAL FRAMEWORK OF THIS AREA

Recently there have been several geochronological investigations in the western part of the IQP in the vicinity of the Brenner Fault and the overlying PCC. Dingeldey et al. (1997) conducted one Ar-Ar stepwise heating experiment on a sample from the western part of the IQP. They found a re-juvenation of the phengite age from 250 Ma to 35 Ma, indicating that the temperature of the Eo-Alpine metamorphic overprint probably exceeded 350°C in this area. Ar-Ar and Rb-Sr dating has been performed on samples from the Brenner area by Rockenschaub et al. (1999). The Ar-Ar plateau ages (206-268 Ma) and Rb-Sr ages (229-255 Ma) of phengites from porphyritic orthogneisses within the IQP, as well as one monazite microprobe age (280±25 Ma), gave indications for a pervasive Permian event (Rockenschaub et al., 1999). They also obtained Eo-Alpine Ar-Ar ages of 135 Ma for synkinematically grown phengites from the dominant foliation S2 in the northern and central parts of the IQP. This result might indicate the onset of the Eo-Alpine metamorphic event and hence put an age constraint on the earliest stage of the Eo-Alpine deformation. While these ages show considerable spread due to incomplete reset-

ting and partial mineral growth during the Eo-Alpine orogeny, these results represent the only absolute age constraint on Eo-Alpine deformation in this unit. In addition to these metamorphic mineral ages, there are also a few data available on the low temperature cooling history (<300°C), based on fission track measurements. Fügenschuh et al. (1997) obtained two fission track ages on zircon from the western part of the IQP, which yielded ages of 42 and 67 Ma. A fission track age on apatite yielded 13±2 Ma. This age is similar to the apatite fission track age of 14.3±2.8 Ma, obtained by Grundmann and Morteani (1985).

Satir and Morteani (1978a) conducted the first geochronological investigations of the KG. They obtained a protolith intrusive age of the orthogneisses of 425 Ma based on a Rb-Sr isotope study. Latest protolith intrusive ages based on U/Pb single zircon dating yield 468±1 Ma and 469±2 Ma (Gangl et al., 2005). Satir and Morteani (1978a) applied the Rb-Sr whole rock isochrone method to the KG, which yielded 322±24 Ma, which is clearly Variscan. Additional Rb-Sr data on phengites from the KG yielded cooling ages of 260 and 273 Ma which are clearly Permian. Based on Th-U-Pb model ages of monazite and thorite, Steyrer and Finger (1996) obtained ages of 323±9 and 353±26 Ma. In addition, there are a few data constraining the low-temperature evolution of the KG. Definite Eo-Alpine ages are still missing from the KG, only strongly disturbed Ar-Ar age patterns with Cretaceous ages in the low-temperature increments were observed (Handler et al., 2000). There are two fission track ages of apatites from the study of Grundmann and Morteani (1985), which yielded 14.5±2.2 and 17.6±1.5 Ma. Zircon and apatite ages from Angelmaier et al. (2000) yielded ages of 63-57 Ma and 13±1 Ma.

Muscovite Ar-Ar ages (Handler et al., 2000) from the WS also indicate a pervasive Permian metamorphic overprint at 267±6 Ma. In addition Angelmaier et al. (2000) obtained Ar-Ar ages of 264±11 Ma, which correlates very well with the age of Handler et al. (2000). Ar-Ar ages from the central Greywacke Zone yielded 102-98 Ma (Schmidlechner et al., 2006), Rb-Sr ages and K-Ar close to Zell am See yielded 137-127 Ma and 113-92 Ma from Zell am See give reasonable evidence for a rejuvenation during a pervasive early Alpine metamorphic overprint around ca. 300°C (Kralik et al., 1987). One zircon and one apatite fission track age available from WS yielded 116±4 Ma and 38±5 Ma, respectively (Angelmaier et al., 2000) which is in disagreement with the Ar-Ar data from Schmidlechner et al. (2006). Clearly more zircon fission track data are needed for this unit.

Compiling the published muscovite Ar-Ar data (Handler et al., 2000; Schmidlechner et al. 2006), biotite Rb-Sr data (Satir and Morteani, 1978a,b), zircon fission track ages (Angelmaier et al., 2000) and apatite fission track data (Grundmann and Morteani, 1985; Angelmaier et al., 2000; Fügenschuh, 1995) and combining them with the available *P-T* estimates from these basement nappes north of the Tauern Window, allows constraints to be placed on the tectonometamorphic evolution of the three units (Piber and Tropper, 2010). While D<sub>1</sub> is clearly

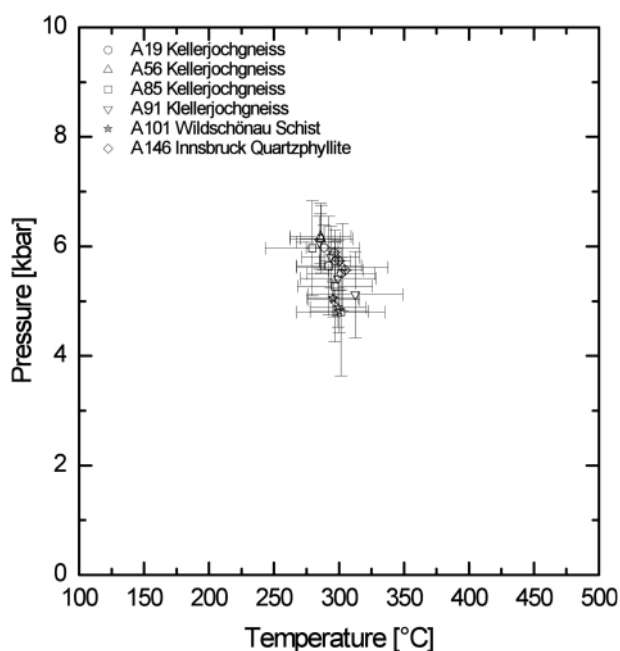


FIGURE 11: Best constrained geothermobarometric results of the IQP, KG and WS with TWQ v.1.02 in the system KNFMASH with the extended dataset of Massonne (1997).

related to a pre-Alpine event of probably Variscan or Permian age,  $D_2$  can unambiguously be attributed to the early stages of the Eo-Alpine event, although definite Eo-Alpine ages are very rare due to the low-temperature nature of the overprint and thus incomplete resetting of the isotope systems (Handler et al., 2000). Since the closure temperature of the zircon fission track system is ca. 260-220°C, this puts time constraints on the last stages of ductile ( $D_4$ ) and/or semiductile ( $D_5$ ) deformation. These data establish that all three units experienced temperatures of 300-400°C at pressures ranging from 4 kbar to 7 kbar at around 135-90 Ma, based on available Ar-Ar and Rb-Sr age data (Rockenschaub et al., 1999).

Concerning the correlation to the structural sequence of Kolenprat et al. (1999) and Piber and Tropper (2010) and the ages of synkinematically grown phengites, ductile deformation in the area of investigation ( $D_2$ - $D_4$ ) probably took place during the Eo-Alpine tectono-metamorphic event. These conditions prevailed until approximately 40-60 Ma when the zircon fission track ages indicate temperatures <220-260°C. Probably around this time, semi-ductile deformation ( $D_5$ ) took place which is in agreement with the proposed tectonic model of Kolenprat et al. (1999).

Compiling the available recent  $P$ - $T$  estimates from the Austroalpine nappes north of the Tauern Window based on the data from this study and Piber and Tropper (2003a,b, 2005, 2007) and Piber et al. (2008, 2009) yields a complex metamorphic evolution of these units. Based on geochronological evidence and the low temperature nature of the Eo-Alpine metamorphic overprint from this investigation the  $P$ - $T$  data of metapelites and the greenschists from the eastern IQP correspond to the Eo-Alpine metamorphic overprint. In contrast, in the western IQP (near Innsbruck), geochronological data point to a pervasive Permian metamorphic event (Piber and Tropper, 2007) and local Eo-Alpine re-juvenation (Fügenschuh, 1995; Handler et al., 2000; Angermaier et al., 2000). This Permian metamorphic overprint corresponds to the formation of Ca-poor plagioclase rims and garnets in garnet micaschists of the central western part (Rockenschaub et al., 2003). In contrast, plagioclase zonation in the biotite-micaschist of the IQP directly underneath the PCC shows Na-rich cores and Ca-rich rims, corresponding to the Eo-Alpine metamorphic overprint, which has also been found in the PCC (Rockenschaub et al., 2003; Piber et al., 2008). Thus would be indicative that the  $P$ - $T$  results obtained of the biotite-micaschists underneath the PCC reflect an Eo-Alpine metamorphic overprint under high greenschist-facies to epidote-amphibolite-facies whereas the central western part of the IQP, represented by the garnet-micaschists, show evidence for a Permian thermal accentuated event (Piber and Tropper, 2007). Consideration of geothermobarometric and mineral age data of the PCC and the underlying biotite micaschists (now IQP) suggests thrusting onto the central part of the IQP during late Cretaceous times (Rockenschaub et al., 1999).

## 9. CONCLUSIONS

U/Pb zircon age constraints and geochemical data of the KG

are in very good agreement with the ages of metaporphic rocks of the Greywackezone (Gangl et al., 2005). This supports an Upper Austroalpine position of this unit according to Schmid et al. (2004) contrary to Tollmann (1977) who postulated the KG to be of Middle Austroalpine origin. The similar time temperature-evolution and the evidence of similar structural evolution of the IQP, the KG and the WS, considering mineral age data from the authors Satir and Morteani (1978), Grundmann and Morteani (1985), Krumm et al. (1987), Fügenschuh (1995), Rockenschaub and Kolenprat (1999), Angermaier et al. (2000) and Handler et al. (2000), and structural investigations of Fügenschuh (1995), Kolenprat and Rockenschaub (1999) and Piber and Tropper (2010) indicate a similar Eo-Alpine tectonic evolution of these three units. The geothermobarometric estimates indicate that the IQP, KG and WS also seem to have been in similar crustal positions during the low-grade Eo-Alpine metamorphic overprint. The  $P$ - $T$  conditions of 290-400°C and 4-7 kbar also indicate that the Eo-Alpine metamorphic overprint possibly took place in a geodynamic setting with a moderate to low geotherm.

## ACKNOWLEDGEMENTS

The authors wish to thank the Austrian Science Fund FWF for financial support in the course of project P14571-B06. Edgar Mersdorf and Bernhard Sartory are thanked for their help with electron microprobe analysis. The constructive comments of the two journal reviewers Christoph Hauzenberger and Thorsten Nagel and the editorial handling by Walter Kurz are greatly appreciated.

## REFERENCES

- Ampferer, O. and Ohnesorge, T., 1918. Geologische Spezialkarte der Österreichisch-Ungarischen Monarchie, 1:75000, Blatt Rattenberg (5048), Wien, Geologische Reichsanstalt.
- Ampferer, O. and Ohnesorge, T., 1924. Erläuterungen zur geologischen Spezialkarte der Republik Österreich, 1:75000, Blatt Innsbruck-Achensee (5047), Geologische Bundesanstalt, Wien.
- Angermaier, P., Frisch, W. and Dunkl, I., 2000. Thermochronological constraints for the TRANSALP section of the Tauern Window. 2<sup>nd</sup> international TRANSALP-Colloquium, Munich, 17.
- Berman, R.G., 1988. Internally-consistent thermodynamic data for minerals in the system  $\text{SiO}_2$ - $\text{K}_2\text{O}$ - $\text{Na}_2\text{O}$ - $\text{Fe}_2\text{O}_3$ - $\text{TiO}_2$ - $\text{Al}_2\text{O}_3$ - $\text{FeO}$ - $\text{MgO}$ - $\text{K}_2\text{O}$ - $\text{H}_2\text{O}$ - $\text{CO}_2$ . *Journal of Petrology*, 29, 445-522.
- Berman, R.G., 1991. Thermobarometry using multi-equilibrium calculations: a new technique with petrological applications. *Canadian Mineralogist*, 29, 833-855.
- Bjerg, S.C., Mogessie, A. and Bjerg, E., 1992. Hyper Form-A hypercard program for the Mac Intosh Microcomputers to calculate mineral formulae from electron microprobe and wet chemical analyses, *Computers and Geosciences*, 18, 717-745.

- Bleibinhaus, F. and Gebrande, H., 2006. Crustal structure of the Eastern Alps along the TRANSALP profile from wide-angle seismic tomography. *Tectonophysics*, 414, 51-69.
- Castellarin, A., Nicolich, R., Fantoni, R., Cantelli, L., Sella, M. and Selli, L., 2006. Structure of the lithosphere beneath the Eastern Alps (southern sector of the TRANSALP transect). *Tectonophysics*, 414, 259-282.
- Collins, E., Hoschek, G. and Mostler, H., 1980. Geologische Entwicklung und Metamorphose im Westabschnitt der nördlichen Grauwackenzone unter besonderer Berücksichtigung der Metabasite. *Mitteilungen der Österreichischen Geologischen Gesellschaft*, 71/72, 343-378.
- Currie, K.L. and van Staal, C.R., 1999. The assemblage stilpnomelane-chlorite-phengitic mica: a geothermobarometer for blueschist and associated greenschist terranes. *Journal of Metamorphic Geology*, 17, 613-620.
- Dingeldey, C., Dallmeyer, D. R., Koller, F. and Massonne H. J., 1997. P-T-t history of the Lower Austroalpine Nappe Complex in the „Tarntaler Berge“ NW of the Tauern Window: implications for the geotectonic evolution of the central Eastern Alps. *Contributions to Mineralogy and Petrology*, 129, 1-19.
- Evans, B.W., 1990. Phase relations of epidote blueschists. *Lithos*, 25, 3-23.
- Froitzheim, N., Schmid, S. M. and Conti, P., 1994. Repeated change from crustal shortening to orogenparallel extension in the Austroalpine units of Graubünden, *Eclogae Geologicae Helvetiae*, 87, 559-612.
- Fügenschuh, B., 1995. Thermal and kinematic history of the Brenner area (Eastern Alps, Tyrol). Unpublished Ph.D Thesis, ETH Zürich, 155 p.
- Fügenschuh, B., Seward, D. and Mancktelow, N., 1997. Exhumation in a convergent orogen: the western Tauern Window. *Terra Nova*, 9, 213-217.
- Gangl, S., Piber, A., Tropper, P., Klötzli, U., Finger, F. and Mirwald, P.W. 2005. Geochronological Evidence for Lower Ordovician Magmatism in the Crystalline Nappes North of the Tauern Window. *Geophysical Research Abstracts*, 7, 03975.
- Grasbon, B., 2001. Großmassenbewegungen im Grenzbereich Innsbrucker Quarzphyllit, Kellerjochgneiss, Wildschönauer Schiefer Finsinggrund (vorderes Zillertal). Unpublished MSc. Thesis, University of Innsbruck, 141 p.
- Grundmann, G. and Morteani, G., 1985. The young uplift and thermal history of the central eastern Alps (Austria, Italy), evidence from apatite fission track ages. *Jahrbuch der Geologischen Bundesanstalt*, 128, 197-216.
- Gwinner, M.P., 1971. *Geologie der Alpen*. Stuttgart, Schweizerbart'sche Verlagsbuchhandlung, 477 p.
- Haditsch, G. and Mostler, H., 1982. Zeitliche und stoffliche Gliederung der Erzvor-kommen im Innsbrucker Quarzphyllit. *Geologisch Paläontologische Mitteilungen der Universität Innsbruck*, 12, 1-40.
- Haditsch, G. and Mostler, H., 1983. The succession of ore mineralization of the lower Austroalpine Innsbruck quartz phyllite. In: Schneider, H.J. (ed.): *Mineral deposits in the Alps*, Springer Verlag, Berlin-Heidelberg-New York, 1-40.
- Handler, R., Genser, J., Freidl, G., Heidorn, R., Neubauer, F., Fritz, H. and Tenczer, V., 2000.  $^{40}\text{Ar}$ - $^{39}\text{Ar}$  ages of white mica from Austroalpine basement units along the TRANSALP section: Tectonic implications. 2<sup>nd</sup> international TRANSALP Colloquium, Munich, 17.
- Hey, M.J., 1954. A new review of the chlorites. *Mineralogical Magazine*, 30, 277-292.
- Holland, T.J.B. and Powell, R., 1998. An internally-consistent thermodynamic data set for phases of petrological interest. *Journal of Metamorphic Geology*, 8, 89-124.
- Holland, T.J.B., Baker, J., and Powell, R., 1998. Mixing properties and activity-composition relationships of chlorites in the system  $\text{MgO-Al}_2\text{O}_3\text{-SiO}_2\text{-H}_2\text{O}$ . *European Journal of Mineralogy*, 10, 395-406.
- Höll, R. and Maucher, A., 1968. Genese und Alter der Scheelit-Magnessit-Lagerstätte Tux in Tirol. *Bayrische Akademie der Wissenschaften, Sitzungsberichte, Mathematisch-Naturwissenschaftliche Klasse*, 1967, 1-11.
- Hoschek, G., Kirchner, E. C., Mostler, H. and Schramm, J. M., 1980. Metamorphism in the Austroalpine units between Innsbruck and Salzburg (Austria)-a synopsis. *Mitteilungen der Österreichischen Geologischen Gesellschaft*, 71/72, 335-341.
- Kolenprat, B., Rockenschaub, M. and Frank, W., 1999. The tectonometamorphic evolution of Austroalpine units in the Brenner Area (Tirol, Austria)-structural and tectonic implications. *Tübinger Geowissenschaftliche Arbeiten, Serie A*, 52, 116-117.
- Kralik, M., Krumm, H. and Schramm, J.M., 1987. Low Grade and Very Low Grade Metamorphism in the Northern Calcareous Alps and in the Greywacke Zone: Illite Crystallinity Data and Isotopic Ages. In: Flügel, H.W. and Faupl, P. (eds.): *Geodynamics of the Eastern Alps*. Deuticke, Vienna, 164-178.
- Leake, B.E. et al., 1997. Nomenclature of amphiboles, Report of the Subcommittee on Amphiboles of the International Mineralogical Association, Commission on New Minerals and Mineral Names. *American Mineralogist*, 82, 1019-1037.
- Lüschen, E., Lammerer, B., Gebrande, H., Millahn, K., Nicolich, R. and TRANSALP Working Group, 2004. Orogenic structure of the Eastern Alps, Europe, from TRANSALP deep seismic reflection profiling. *Tectonophysics*, 388, 85-102.

- Massonne, H.J. and Szpurka, Z., 1997. Thermodynamic properties of white micas on the basis of high-pressure experiments in the system  $K_2O$ - $MgO$ - $Al_2O_3$ - $SiO_2$ - $H_2O$  and  $K_2O$ - $FeO$ - $Al_2O_3$ - $SiO_2$ - $H_2O$ , *Lithos*, 41, 229-250.
- Massonne, H.J. and Kopp, J., 2005. A low-variance mineral assemblage with talc and phengite in an eclogite from the Saxonian Erzgebirge, Central Europe, and its P-T evolution. *Journal of Petrology*, 46, 355-375.
- McMullin, D.W.A., Berman, R. G. and Greenwood, H.J., 1991. Calibration of the SGAM thermobarometer for pelitic rocks using data from phase-equilibrium experiments and natural assemblages. *Canadian Mineralogist*, 29, 889-908.
- Mogessie, A., Ettinger, K., Leake, B. E. and Tessadri, R., 2001. AMPH-IMA97: a hypercard program to determine the name of an amphibole from electron microprobe and wet chemical analyses. *Computers and Geosciences*, 27, 1169-1178.
- Mostler, H., Heissel, G. and Gasser, G., 1982. Untersuchung von Erzlagerstätten im Innsbrucker Quarzphyllit und auf der Alpeiner Scharte. *Archiv für Lagerstättenforschung der Geologischen Bundesanstalt, Wien*, 1, 77-83.
- Ortner, H. and Reiter, 1999. Kinematic history of the Triassic South of the Inn Valley (Northern Calcareous Alps, Austria) – Evidence for Jurassic and Late Cretaceous large scale faulting. 3<sup>rd</sup> Workshop on Alpine Geological Studies, Biella, Oropa.
- Ortner, H., Brandner, R. and Gruber, A., 1999. Kinematic evolution of the Inn Valley Shear Zone from Oligocene to Miocene. *Tübinger Geowissenschaftliche Arbeiten Serie A*, 52, 192-193.
- Piber, A., 2002. Tectonometamorphic evolution of the Austro-Alpine nappes in the northern Zillertal-Area, Eastern Alps. Unpublished MSc. Thesis, University of Innsbruck, 268 p.
- Piber A., 2005. The metamorphic evolution of the Austroalpine nappes north of the Tauern Window (Innsbruck Quartzphyllite Complex-Patscherkofel Crystalline Complex -Kellerjochgneiss and Wildschönau Schists). Unpublished Ph.D. Thesis, University of Innsbruck, 261 p.
- Piber, A. and Tropper, P., 2003a. Preliminary Eo-Alpine thermobarometric results of the Austroalpine crystalline basement nappes in the northwest of the Tauern Window between the Zillertal and the Wipptal (Eastern Alps, Tyrol). *Arbeitstagung der Geologischen Bundesanstalt*, 2003, 59-65.
- Piber, A. and Tropper, P., 2003b. Multi-equilibrium thermobarometry in low grade metamorphic rocks from the Austroalpine nappes north of the Tauern Window (Kellerjochgneiss, Innsbruck Quartzphyllite). *Memorie di Scienze Geologiche*, 54, 227-231.
- Piber, A. and Tropper, P., 2005. The polymetamorphic evolution of the Austroalpine Innsbruck Quartzphyllite Complex, *Mitteilungen der Österreichischen Mineralogischen Gesellschaft*, 151, 103.
- Piber, A. and Tropper, P., 2007. Muscovite-chlorite-quartz thermobarometry of the Permian metamorphic overprint of the central part of the western Innsbruck Quartzphyllite Complex (Tyrol, Austria). *Mitteilungen der Österreichischen Mineralogischen Gesellschaft*, 153, 291-300.
- Piber, A. and Tropper, P., 2010. Tectonometamorphic evolution of the Austroalpine nappes in the northern Zillertal area (Tyrol, Eastern Alps). *Geo.Alp*, 7, 71-92.
- Piber, A., Tropper, P. and Mirwald, P.W., 2008. The metamorphic evolution of the Patscherkofel Crystalline Complex (Tyrol, Eastern Alps, Austria). *Austrian Journal of Earth Sciences*, 101, 27-35.
- Piber, A., Tropper, P. and Mirwald, P.W., 2009. Geothermobarometry of a stilpnomelane-garnet-bearing metapegmatite: P-T constraints on the Eo-Alpine metamorphic overprint of the Austroalpine nappes north of the Tauern Window. *Mineralogy and Petrology*, 96, 99-111.
- Pichler, A., 1868. *Beiträge zur Geognosie Tirols*. Jahrbuch der Geologischen Reichsanstalt, Wien.
- Powell, R., 1978. *Equilibrium thermodynamics in petrology*. Harper and Row, London. 284 p.
- Powell, R. and Holland, T.J.B., 1988. An internally consistent thermodynamic data set with uncertainties and correlations: 3. Application methods, worked examples and a computer program. *Journal of Metamorphic Geology*, 6, 173-204.
- Powell, R. and Holland, T.J.B., 1994. Optimal geothermometry and geobarometry. *American Mineralogist*, 79, 120-133.
- Reiter, F., 2000. *Strukturell-stratigraphische Neubearbeitung der Schwazer Trias westlich des Zillertales*. Unpublished Masters Thesis, University of Innsbruck, 176 p.
- Reitz, E. and Höll, R., 1991. Biostratigraphischer Nachweis von Arenig in der Nördlichen Grauwackenzone (Ostalpen). *Jahrbuch der Geologischen Bundesanstalt*, 134/2, 329-344.
- Rockenschaub, M., Kolenprat, B. and Frank, W., 1999. The tectonometamorphic evolution of Austroalpine units in the Brenner area (Tirol, Austria)-new geochronological implications. *Tübinger Geowissenschaftliche Arbeiten Serie A*, 52, 118-119.
- Rockenschaub, M., Kolenprat, B. and Nowotny, A., 2003. Innsbrucker Quarzphyllitkomplex, Tarntaler Mesozoikum, Patscherkofelkristallin. *Arbeitsberichte zur Arbeitstagung der Geologischen Bundesanstalt in Trins im Gschnitztal* 2003, 41-58.
- Roth, R., 1983. *Petrographie und Tektonik der mittelostalpinen Kellerjochgneis-Decke und angrenzender Gebiete zwischen Schwaz und Märzengrund (Tirol.)* Unpublished Ph.D. Thesis, University of Münster, 196 p.

- Sassi, F.P. and Spiess, R., 1992. Further Data on pre-Alpine metamorphic pressure conditions of the Austridic phyllitic complexes in the Eastern Alps. In: Carmignagi, L. and Sassi, F.P. (eds.), Contributions to Geology of Italy with special regard to the Paleozoic basements. IGCP Mo. 276, Newsletter 5, 297-307.
- Satir, M. and Morteani, G., 1978a. Kaledonische, herzynische und alpidische Ereignisse im Mittelostalpin nördlich der westlichen Hohen Tauern abgeleitet aus petrographischen und geochronologischen Untersuchungen, Geologische Rundschau, 68, 1-40.
- Satir, M. and Morteani, G., 1978b. *P-T* conditions of the high-pressure Hercynian event in the Alps as deduced from petrological, Rb-Sr and  $O^{18}/O^{16}$  data on phengites from the Schwazer Augengneise (EASTERN ALPS, AUSTRIA), Schweizerische Mineralogische und Petrographische Mitteilungen, 58, 289-301.
- Satir, M., Friedrichsen, H. and Morteani, G., 1980.  $^{18}O/^{16}O$  and D/H study of the minerals from the Steinkogelschiefer and the Schwazer Augengneis (Salzburg/Tirol, Austria), Schweizerische Mineralogische und Petrographische Mitteilungen, 60, 99-109.
- Schauder, P., 2002. Ordovizische Entwicklung im Westabschnitt der Nördlichen Grauwackenzone unter besonderer Berücksichtigung mafischer und ultramafischer Magmatite. Geochemische, Isotopengeochemische und geochronologische Untersuchungen. Münchner Geologische Hefte, 30, 103 p.
- Schmid, S.M., Fügenschuh, B., Kissling, E. and Schuster, R., 2004. Tectonic map and overall architecture of the Alpine orogen. *Eclogae Geologicae Helvetiae*, 97, 93-117.
- Schmidegg, O., 1954. Achsen- und Flächengefüge beiderseits des Silltalbruches zwischen Innsbruck und Matrei, Tschermaks Mineralogische und Petrographische Mitteilungen, 4, 125-137.
- Schmidegg, O., 1964. Die Ötztaler Schubmasse und ihre Umgebung. *Verhandlungen der Geologischen Bundesanstalt*, 1957/1, 76-77.
- Schmidlechner, M., Neubauer, F. and Handler, R., 2006. Extent and age of metamorphism of the central Grauwacken Zone, Eastern Alps: a Ar-Ar study, *Pangeo 2006*, Innsbruck University Press, 314-315.
- Schönlaub, H.P., 1979. Das Paläozoikum in Österreich. *Abhandlungen der Geologischen Bundesanstalt*, 33, 1-124.
- Schönlaub, H.P., 1980. Die Grauwackenzone In: OBERHAUSER, R. (ed.): *Der geologische Aufbau Österreichs*. Springer, Wien, 699 p.
- Söllner, F., Miller, H. and Höll, R., 1997. Alter und Genese der rhyodazitischen Metavulkanite ("Porphyroide") der Nördlichen Grauwackenzone und der Karnischen Alpen (Österreich): Ergebnisse von U/Pb Zirkondatierungen. *Zeitschrift der Deutschen Geologischen Gesellschaft*, 148/3-4, 499-522.
- Steyrer, H.P. and Finger, F., 1996. Der Schwazer Augengneis: ein östlicher Ausläufer des Ötztal Kristallins? *Mitteilungen der Österreichischen Mineralogischen Gesellschaft*, 141, 226-227.
- Tollmann, A., 1963. *Ostalpensynthese*, Franz Deuticke, Vienna, 256 p.
- Tollmann, A., 1977. *Geologie von Österreich, Bd.1, Die Zentralalpen*, Franz Deuticke, Vienna, 766 p.
- Tollmann, A., 1986. *Geologie von Österreich, Bd.3., Gesamtübersicht*, Franz Deuticke, Vienna, 718 p.
- TRANSALP WORKING GROUP, 2002. First deep seismic reflection images of the Eastern Alps reveal giant crustal wedges and transcrustal ramps. *Geophysical Research Letters*, Vol. 29, No.10, 10.1029/2002GL014911, 2002.
- Willner, A.P., Herve, F. and Massonne, H.J., 2000. Mineral chemistry and pressure-temperature evolution of two contrasting high-pressure-low-temperature belts in the Chronos Archipelago, Southern Chile. *Journal of Petrology*, 41, 309-330.

Received: 12 March 2012

Accepted: 12 November 2012

Peter TROPPE<sup>1</sup> & Andreas PIBER

Institute of Mineralogy and Petrography, Faculty of Geo- and Atmospheric Sciences, University of Innsbruck, Innrain 52f, A-6020 Innsbruck, Austria;

<sup>1</sup> Corresponding author, peter.tropper@uibk.ac.at